

Li insertion/extraction characteristics of a vacuum-deposited Si–Sn two-component film

Motohisa Suzuki^{a,*}, Junji Suzuki^a, Kyoichi Sekine^a, Tsutomu Takamura^b

^a Department of Chemistry, Rikkyo University, 3-34-1 Nishiikebukuro, Toshimaku, Tokyo 171-8501, Japan

^b Department of Applied Chemistry, Harbin Institute of Technology, 92 West Dazhi Street, Harbin 150001, China

Available online 24 May 2005

Abstract

Vacuum-deposited Si–Sn two-component films were prepared by depositing Si and Sn simultaneously on a metal foil substrate. The composition of the films was estimated from the ratio of consumption of the two evaporation sources. SEM and XRD revealed the film structure consisting of two different phases, where Sn nanoparticles were dispersed homogeneously in the amorphous Si matrix. The film with higher Sn content gave unsatisfactory results, which is in contrast to the much improved results obtained with a film containing less Sn. The conductivity of the Si–Sn film was found to be higher than that of a pure Si film, which was attributed to the homogeneously deposited Sn nanoparticles. This enabled us to realize a discharge capacity of 400 mAh g⁻¹ even after 500 charge/discharge cycles at a very high rate of 20 C.

© 2005 Published by Elsevier B.V.

Keywords: Si–Sn two-component film; Vacuum-deposited film; High rate charge/discharge performance; Nano scale size dispersion; High capacity anode; Li insertion/extraction

1. Introduction

In response to the high demand for advanced portable electronic equipment, numerous studies have been conducted on active materials for Li-ion batteries in view of enlarging the Li accommodation capacity [1]. Attempts have been made to replace commonly used graphitized anode materials having a theoretical capacity of 372 mAh g⁻¹ by Si materials, which have an extraordinarily large Li accommodation capacity, as high as over 4000 mAh g⁻¹ [2]. A great shortcoming of Si is its large volume expansion during Li insertion which leads to a reduced cycle life due to the crystal collapse. Several effective methods have been proposed to prevent the capacity decrease, involving the use of Si composites [3], nano-structured Si [4], amorphous Si [5,6], thin Si films fabricated by sputtering [7], and pillar structures [8].

We proposed vacuum deposition to fabricate a thin Si film on a metal foil substrate, which showed satisfactory

cycle performance whenever the film is not thick [9,10]. The thicker film, however, gave depressed performance. This was found to attribute to the decreased electric conductivity of the thicker film. The reason for this remains unclear, but we were able to improve performance by using impurity doped Si as evaporation source, in which case the original conductivity was as high as 10⁶ orders of magnitude higher than that of the intrinsic Si crystal [10]. The high rate capability, however, did not improve appreciably.

Here in this study, we would like to provide a novel method to improve the conductivity by depositing a two-component film where a substance having a high conductivity is incorporated. Practically in the present study, we prepared a film consisted of a Si matrix and Sn nanoparticles dispersed homogeneously within the Si matrix. Vacuum deposition of the two-component film was performed by simultaneous evaporation of Si and Sn from separate evaporation sources. The homogeneously dispersed conductive Sn particles yielded a highly conductive Si film. We chose Sn as a conductivity aid on the basis of results reported by Dahn and coworkers [11].

* Corresponding author. Tel.: +81 3 3985 2363; fax: +81 3 3985 2363.
E-mail address: 041b008z@stu.rikkyo.ne.jp (M. Suzuki).

The Si–Sn (two-component) film comprising an optimal mixture of Si and Sn exhibited a stable cycle performance even under very high charge/discharge rate.

2. Experimental

2.1. Evaporation sources and vacuum deposition method

Si–Sn films of varying thickness were prepared by vacuum deposition under a pressure of 10^{-5} Torr. As a substrate, we used a surface roughened 30 μm -thick Ni foil (etched with a 0.5 mol L^{-1} aqueous FeCl_3 solution for 3 min) [12,13] or a surface roughened 38 μm -thick electrolytic Cu foil (deposited by a special electrolytic method in an aqueous solution of CuSO_4) [14,15]. Negative carrier doped Si wafer ($5 \times 10^{-22} \text{ mol m}^{-3}$ phosphor doped, $5 \Omega \text{ cm}$, Shin-Etsu Chemical Co. Ltd.) granulated, and Sn grains (purity 99.99%, Nilaco Co. Ltd.) were used as evaporation sources. The two evaporation sources were loaded on separate tungsten boats placed in a parallel manner in the vacuum chamber, and heated by supplying power directly to the tungsten boats. The deposition rate was controlled by adjusting the power supply; the amount deposited was monitored by a quartz vibrating microbalance mounted near the substrate. The thickness and atomic ratio Si/Sn of the Si–Sn film were estimated on the basis of the amounts evaporated from the two evaporation sources. The weights of the evaporation sources were measured before and after vacuum deposition; the weight difference was assumed to be proportional to the amount deposited. The composition of the Si–Sn film was adjusted to be Si-rich because the theoretical capacity of Si (4200 mAh g^{-1}) is larger than that of Sn (1000 mAh g^{-1}).

2.2. Electrochemical evaluation

The electrochemical cell was a three-compartment cylindrical Pyrex glass cell (15 ml) where pure metallic Li foils were used as counter and reference electrodes. The metal foil bearing the Si–Sn film was cut into a $1 \text{ cm} \times 1 \text{ cm}$ and used as a test electrode. The electrolyte was a 1:1 (v/v) mixture of ethylene carbonate (EC) and dimethyl carbonate (DMC) containing 1 M LiClO_4 (Tomiya Chemicals; contaminant water was less than 15 ppm). Electrochemical measurements were performed by cyclic voltammetry (CV) at a sweep rate of 1 mV s^{-1} , and repeated constant current charge/discharge tests (CC). All measurements were conducted in a glove box filled with dried argon gas at ambient temperature. X-ray diffraction (XRD) patterns and SEM images were obtained to characterize the Si–Sn film.

3. Results and discussion

3.1. Estimation of the composition of the Si–Sn film

Cyclic voltammograms of a 4800 \AA -thick Si–Sn film (atomic ratio Si:Sn = 7:2) vacuum-deposited on an etched

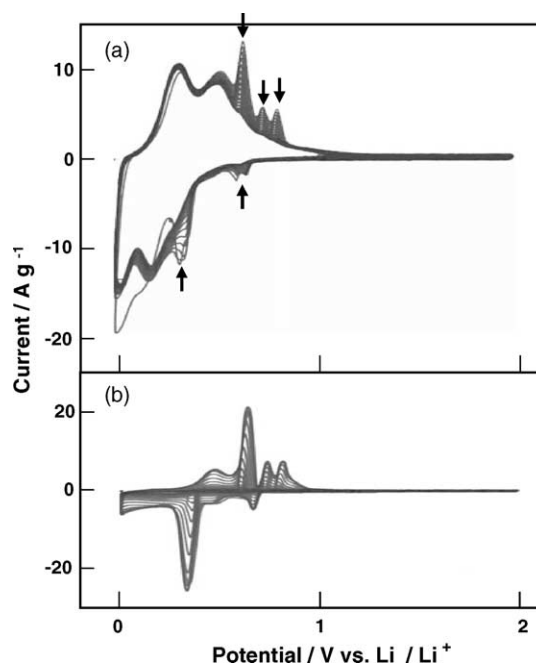


Fig. 1. Cyclic voltammograms of (a) a 4800 \AA -thick Si–Sn film (atomic ratio Si:Sn was 7:2) vacuum-deposited on an etched Ni foil; (b) a 1200 \AA -thick pure Sn film on a nominally identical Ni foil for the initial 20 cycles. Sweep rate: 1 mV s^{-1} .

Ni foil are shown in Fig. 1(a). Two different types of Li insertion and extraction peaks with respect to Si and Sn were observed. The peaks due to insertion and extraction of Li in Si were very stable, while the corresponding peaks for Sn were unstable, showing a gradual depression in height (indicated by arrows), that disappeared after 20 cycles. This degradation is ascribed to the collapse of the Sn microcrystals due to the large volume change associated with the insertion and extraction of Li, resulting in poor electrical contact between particles and the current collector. Similar cycle performance degradation was observed in the case of a vacuum-deposited pure Sn film (Fig. 1(b)). XRD patterns of the Si–Sn film are shown in Fig. 2(b) and (c). XRD peaks of Sn could be identified even after repeated charge/discharge cycles, suggesting that the microcrystals of Sn particles become too loose for supporting electrical contact, resulting in the isolation of the particles from the electrochemical reaction. After 20 cycles, the film showed stable CVs.

The SEM image of the 4800 \AA -thick Si–Sn film is shown in Fig. 3. The image shows a number of small spots dispersed homogeneously over the deposited Si film. Such spots were not observed for the pure silicon film: these spots can be identified as nano-dispersed Sn particles. We will show later that the spot size diminishes with decreasing Sn content (Fig. 5).

The constant current cycle performance of the 4800 \AA -thick Si–Sn film was unsatisfactory. Since we found that the performance was dependent on the Si/Sn ratio, we examined deposited films of varying composition. We found that the film having a reduced amount of Sn gave better cycle performance. Fig. 4 shows the cyclic voltammograms of

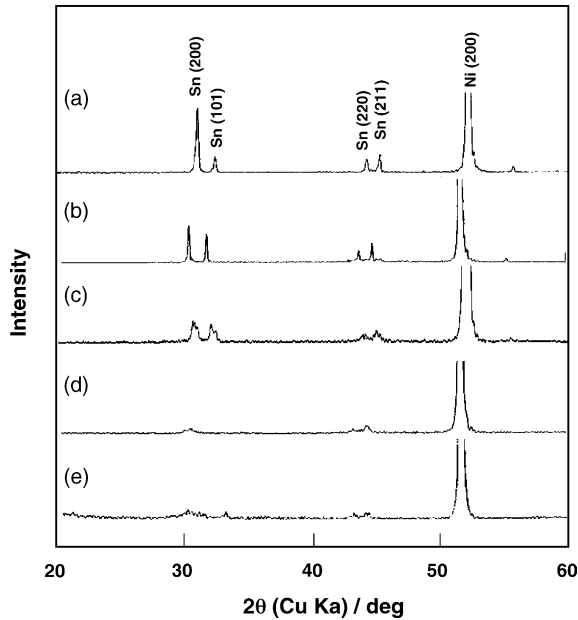


Fig. 2. XRD patterns of films vacuum-deposited on an etched Ni foil: (a) a 1200 Å-thick pure Sn film; (b) a 4800 Å-thick Si–Sn film (atomic ratio Si:Sn was 7:2) before cycle testing; (c) a 4800 Å-thick Si–Sn film after 40 CV cycles; (d) a 3500 Å-thick Si–Sn film (atomic ratio Si:Sn was 8:1) before cycling; (e) a 3500 Å-thick Si–Sn film after 40 CV cycles.

a 3500 Å-thick Si–Sn (atomic ratio Si:Sn = 8:1) vacuum-deposited on an etched Ni foil. Peaks due to Sn could not be identified on CVs, leaving only Si peaks, resulting in very stable performance. The SEM image of this film is shown in Fig. 5, where we see the size of the spots of Sn was remarkably reduced and buried deeper in the Si matrix as compared with those in Fig. 3.

XRD patterns for the sample in Fig. 5 are shown in Fig. 2(d) and (e) before and after 40 charge/discharge cycles, respectively. No distinct peak was observed near 28° where silicon crystal gives a very intense (1 1 1) peak, implying that the deposited film was amorphous [13]. The XRD patterns showed Sn peaks at about 30° and 44° , however,

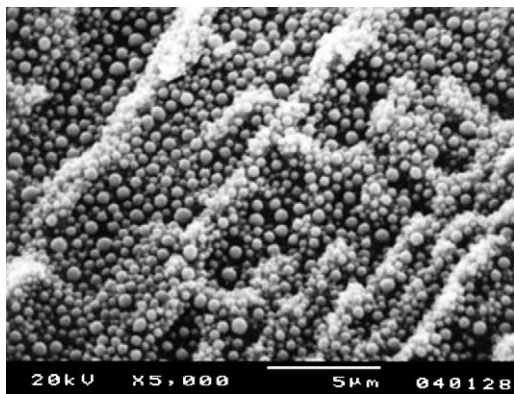


Fig. 3. SEM image of a 4800 Å-thick Si–Sn film (atomic ratio Si:Sn was 7:2) vacuum-deposited on an etched Ni foil, before cycle testing. SEM image reveals small spots of Sn.

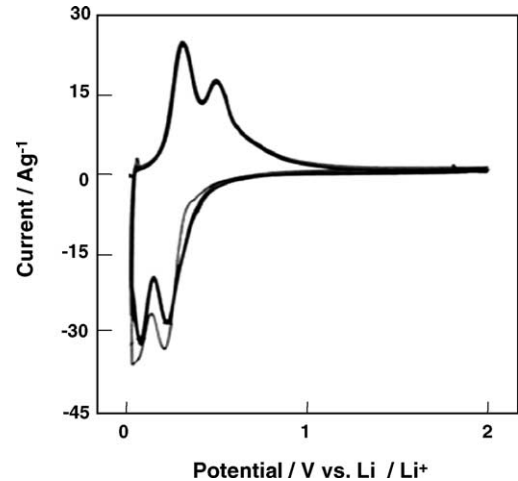


Fig. 4. Cyclic voltammograms of a 3500 Å-thick Si–Sn film (atomic ratio Si:Sn was 8:1) vacuum-deposited on an etched Ni foil for the initial 20 cycles. Sweep rate: 1 mV s^{-1} .

these peaks were broader than that of pure Sn film both before and after the charge/discharge cycles. This may imply that the incorporated Sn in this case was amorphous or in the form of nanoparticles. Thus, the conductivity of this film is expected to be higher and give rise to an excellent high rate charge/discharge performance.

Next, we attempted to evaluate cyclability under a very high charge/discharge rate. We compared the 10C rate cycle performance of a 3500 Å-thick Si–Sn film (atomic ratio Si:Sn = 8:1) and a 3300 Å-thick pure Si film. As can be seen in Fig. 6, the Si–Sn film showed a very high capacity retention even after 500 cycles of charge/discharge under a high rate of 10C. In addition, the initial irreversible capacity of this film was only 12%, which is significantly improved compared with the 26% for a pure Si film. This remarkable improvement in cycle performance can well be attributed to the increase in electrical conductivity of the matrix. We studied the performance of this film under higher charge/discharge rates still. The charge/discharge profiles are shown in Fig. 7. We see that the discharge curve remains smooth, maintaining

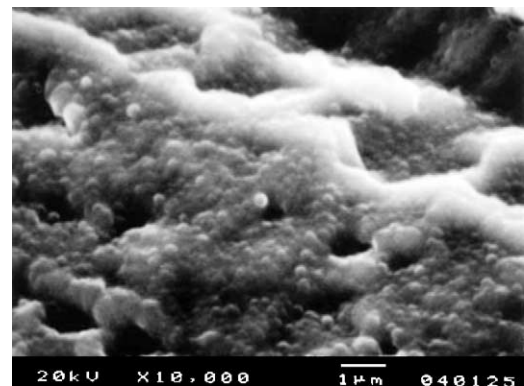


Fig. 5. SEM image of a 3500 Å-thick Si–Sn film (atomic ratio Si:Sn was 8:1) vacuum-deposited on an etched Ni foil before cycle testing. The Sn spots were smaller than those in Fig. 3.

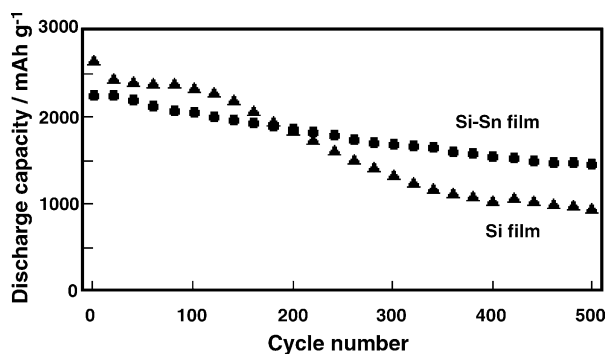


Fig. 6. 10 C rate cycle performance of a 3500 Å-thick Si–Sn film (atomic ratio Si:Sn was 8:1) vacuum-deposited on an etched Ni foil and a 3300 Å-thick pure Si film on a nominally identical Ni foil.

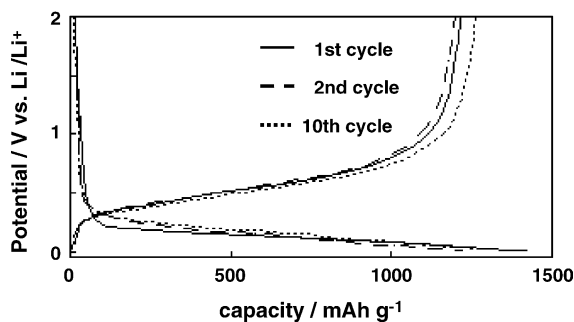


Fig. 7. 30 C rate charge/discharge profiles of a 3500 Å-thick Si–Sn film (atomic ratio Si:Sn was 8:1) vacuum-deposited on an etched Ni foil.

a potential of around 0.5 V, which is acceptable performance for battery applications. Cyclability under very high rates is plotted in Fig. 8, showing that the present film could retain 800 mAh g⁻¹ discharge capacity under a high rate of 30 C even after 500 cycles, while keeping the initial irreversible capacity loss as low as 14%.

3.2. Cycle performance of a thicker Si–Sn film

Since a 3500 Å-thick film is too thin for use in a battery in practice, we tried to fabricate a thicker film on a Cu substrate foil deposited by a special electrolytic technique that yielded a roughened foil surface, enabling the foil to support thick

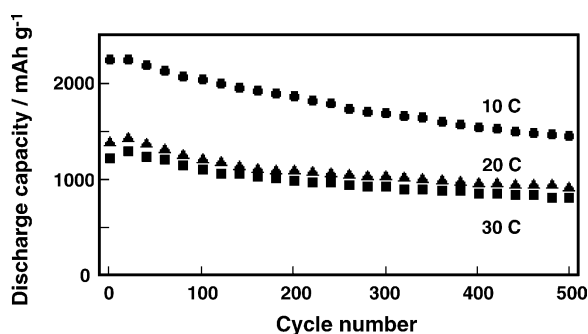


Fig. 8. High rate cycle performance of a 3500 Å-thick Si–Sn film (atomic ratio Si:Sn was 8:1) vacuum-deposited on an etched Ni foil.

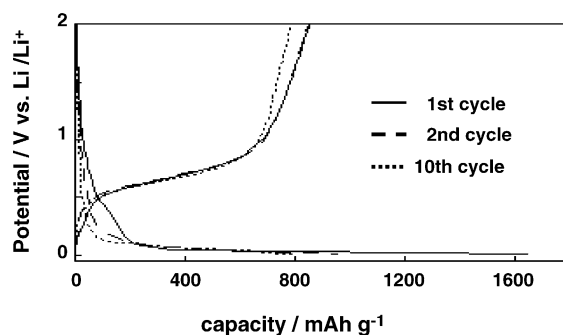


Fig. 9. 20 C rate charge/discharge profiles of a 18,000 Å-thick Si–Sn film (atomic ratio Si:Sn was 13:1) vacuum-deposited on an electrolytic Cu foil.

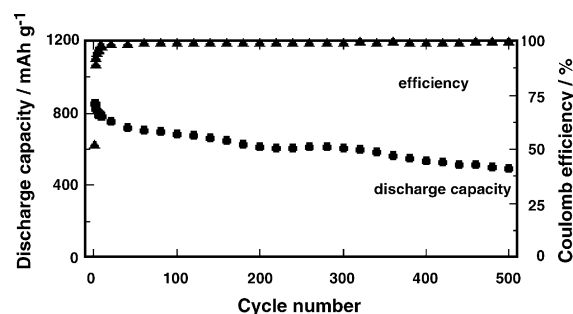


Fig. 10. 20 C rate cycle performance of a 18,000 Å-thick Si–Sn film (atomic ratio Si:Sn was 13:1) vacuum-deposited on an electrolytic Cu foil.

Si films [14,15]. Figs. 9 and 10 show, respectively, the charge/discharge profiles and cyclability obtained for a 18,000 Å-thick film at a rate of 20 C. By contrast, under such heavy current charge/discharge conditions, a pure Si film of the same thickness gave no capacity. Thus, we have successfully demonstrated that the Si–Sn film system can afford to retain a high Li discharge capacity even under an extremely high current charge/discharge cycle test.

4. Conclusion

Vacuum-deposited Si–Sn films were prepared by simultaneous deposition of Si and Sn using two tungsten evaporation boats. In these films, Sn was dispersed in the form of nanoparticles within an amorphous Si matrix, as revealed by SEM and XRD observations. High Sn loading worsened performance. A 3500 Å-thick Si–Sn film (atomic ratio Si:Sn=8:1) showed excellent high rate performance retaining a discharge capacity of over 1400 mAh g⁻¹ even after 500 charge/discharge cycles under 10 C rate loading.

A 18,000 Å-thick Si–Sn film (atomic ratio Si:Sn=13:1) kept over 400 mAh g⁻¹ discharge capacities even after 500 cycles under 20 C rate charge/discharge. This improvement in performance may be attributed to the highly enhanced conductivity owing to the Sn particles dispersed homogeneously in the Si film. In addition, Si–Sn films showed lower initial irreversible capacities than pure Si films. Achieving high conductivity in a Si film is key in imparting a high capacity anode with good cyclability for lithium-ion batteries.

Acknowledgements

The authors extend their heartfelt appreciation to Dr. Mikio Aramata of Shin-Etsu Chemical Co. Ltd. for kindly providing negative carrier doped Si wafers. The authors also thank Nippon Denka Ltd. for their kind provision of specially made electrolytic Cu foils.

References

- [1] J.M. Tarascon, M. Armand, *Nature (London)* 414 (2001) 359.
- [2] J.O. Besenhard (Ed.), *Handbook of Battery Materials*, Wiley-VCH, Weinheim, 1999, pp. 363–380.
- [3] M. Yoshio, H. Wang, K. Fukuda, T. Umeno, N. Dimov, Z. Ogumi, *J. Electrochem. Soc.* 149 (2002) 1598.
- [4] H. Li, X. Huang, L. Chen, G. Zhou, Z. Zhang, D. Yu, Y.J. Mo, N. Pe, *Solid State Ionics* 135 (2000) 181.
- [5] L.Y. Beaulieu, K.W. Eberman, R.L. Turner, L.J. Krause, J.R. Dahn, *Electrochem. Solid State Lett.* 4 (2001) 137.
- [6] S. Bourderau, T. Brousse, D.M. Schleich, *J. Power Sources* 81–82 (1999) 233.
- [7] H. Ikeda, M. Fujimoto, Y. Doumoto, H. Yagi, H. Sakurai, N. Tamura, R. Ohshita, M. Kamino, I. Yonezu, Presented at the Battery Symposium in Japan, Yokohama, Japan, 21–23 November, 2002.
- [8] M. Green, E. Fielder, B. Scrosati, M. Wachtler, J.S. Moreno, *Electrochem. Solid State Lett.* 6 (2003) 75.
- [9] S. Ohara, J. Suzuki, K. Sekine, T. Takamura, *J. Power Sources* 119–121 (2003) 591.
- [10] S. Ohara, J. Suzuki, K. Sekine, T. Takamura, *Electrochemistry* 71 (2003) 1126.
- [11] L.Y. Beaulieu, K.C. Hewitt, R.L. Turner, A. Bonakdarpour, A.A. Abdo, L. Christensen, K.W. Eberman, K.J. Krause, J.R. Dahn, *J. Electrochem. Soc.* 150 (2003) 149.
- [12] M. Uehara, J. Suzuki, K. Sekine, T. Takamura, Presented at the 44th Battery Symposium in Japan, Sakai, Japan, 4–6 November, 2003.
- [13] T. Takamura, S. Ohara, M. Uehara, J. Suzuki, K. Sekine, *J. Power Sources* 129 (1) (2004) 96.
- [14] T. Takamura, M. Uehara, T. Simokawaji, J. Suzuki, K. Sekine, Presented at the 71st Meeting of the Electrochemical Society in Japan, Yokohama, Japan, 24–26 March, 2004.
- [15] T. Takamura, M. Uehara, M. Suzuki, J. Suzuki, K. Sekine, K. Tamura, Presented at the 6th Meeting on Materials for Chemical Batteries in Japan, Tokyo, Japan, 14–15 June, 2004.